Coded Apertures in Compressive Tomography

Gonzalo R. Arce
Charles Black Evans Professor and
Fulbright-Nokia Distinguished Chair

Department of Electrical and Computer Engineering
University of Delaware,
Newark, Delaware, 19716

Tomography Problem

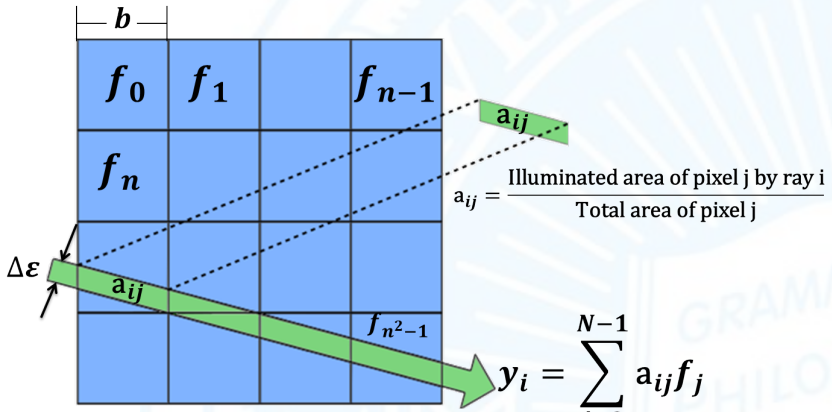

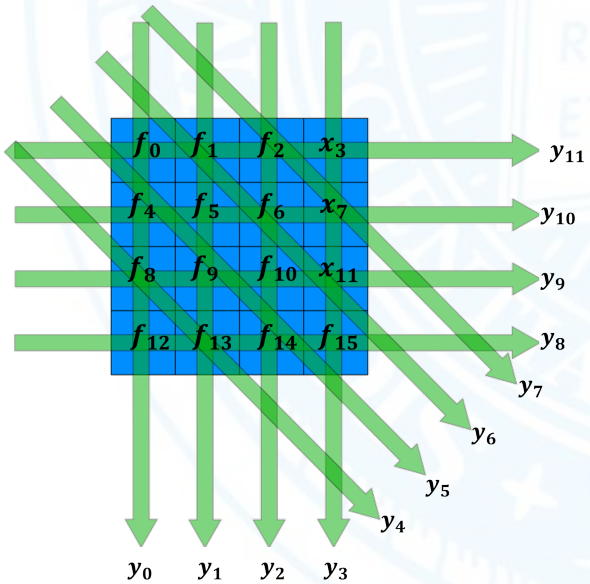

The Inverse Problem

- Matrix **H** is typically almost singular
- Ill-conditioned problem
- No fast inversion method
- Direct Inversions are extremely time- and memory-intensive

New Approach

- Coded Aperture in Compressive X-Ray Tomography

Motivation for Compressive X-Ray Tomography

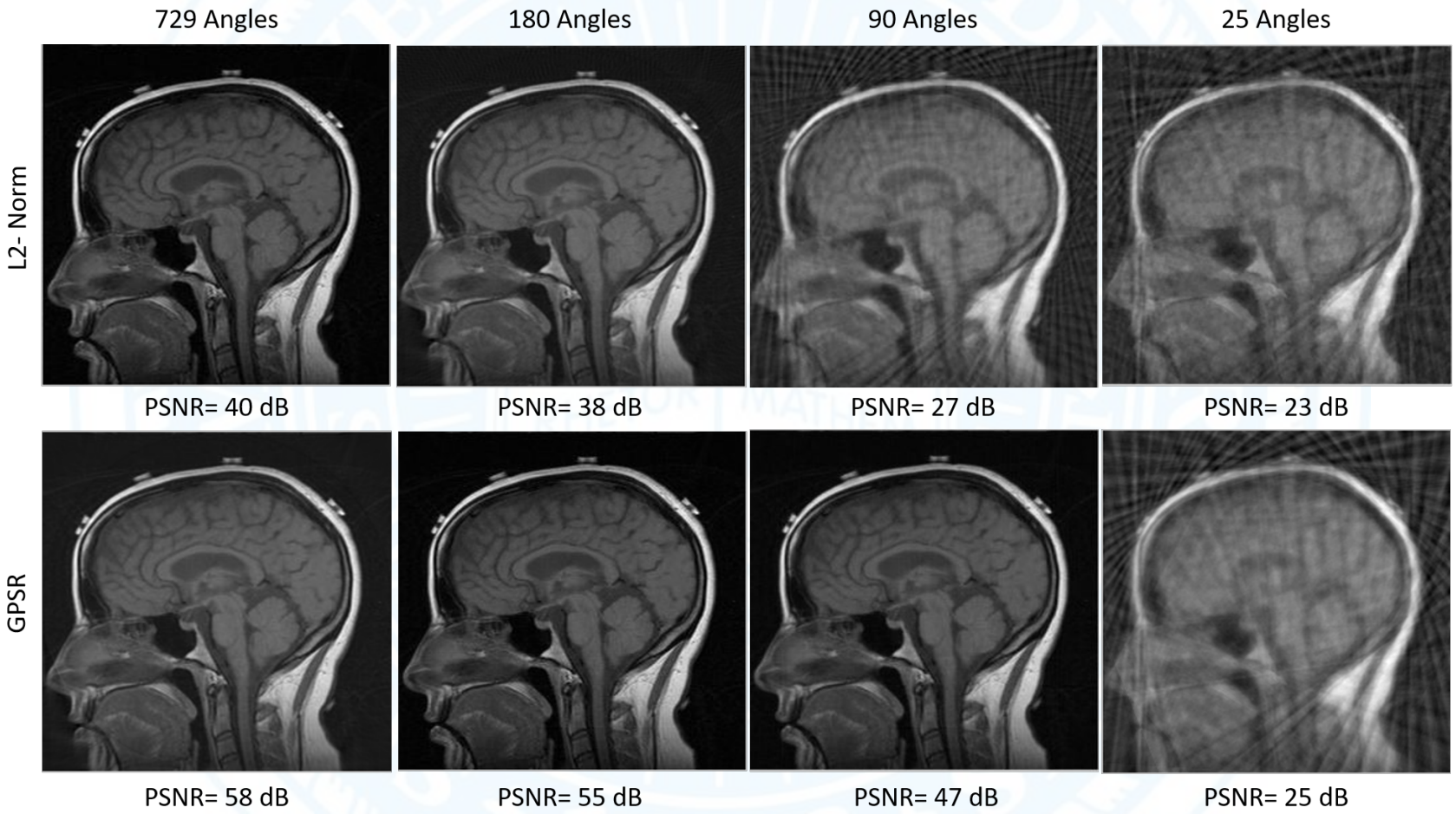

Motivation for Compressive X-Ray Tomography

- Random coded apertures trim down the number of rays.
- **H** matrix has the same size in both cases.

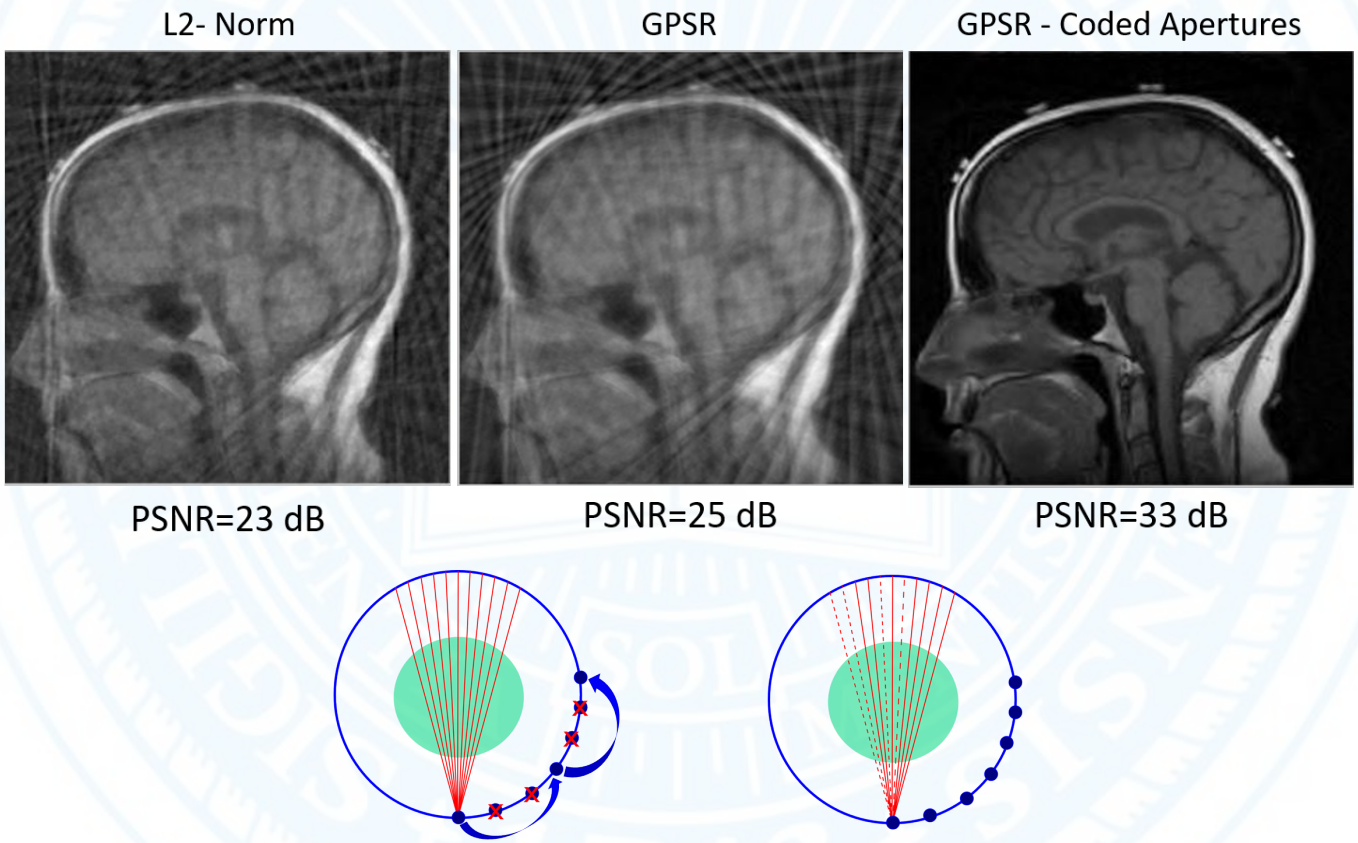

Coded aperture compressive fan beam X-ray CT

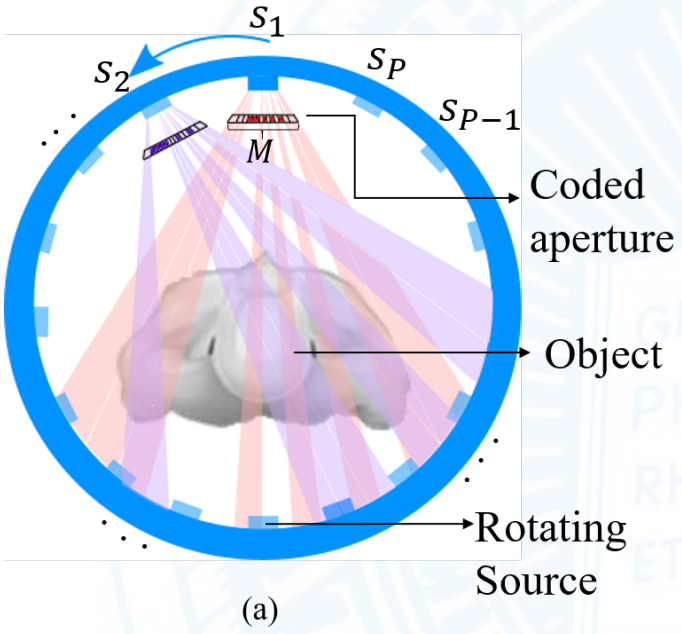

(a)

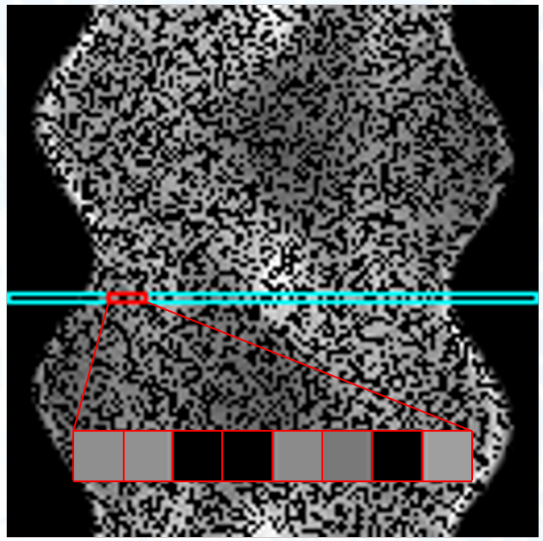

(b)

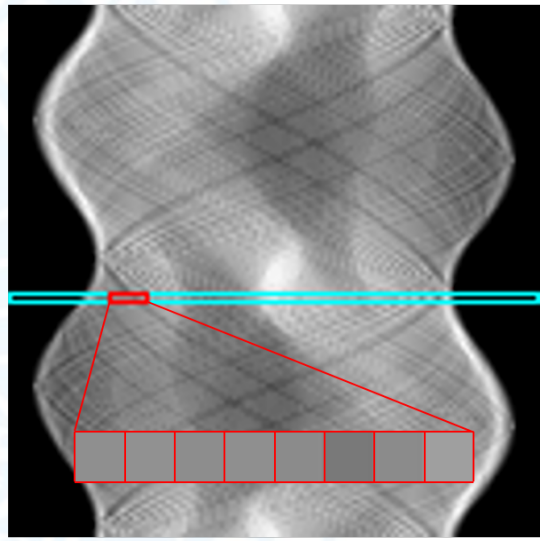

(c)

(a) Coded aperture compressive fan beam X-ray CT system.

(b) Undersampled sinogram of 64×64 Shepp-Logan Phantom $P = 128$, $M = 128$, 50% undersampling.

(c) Complete uncoded sinogram.

All ones - Coded aperture and energy mapping

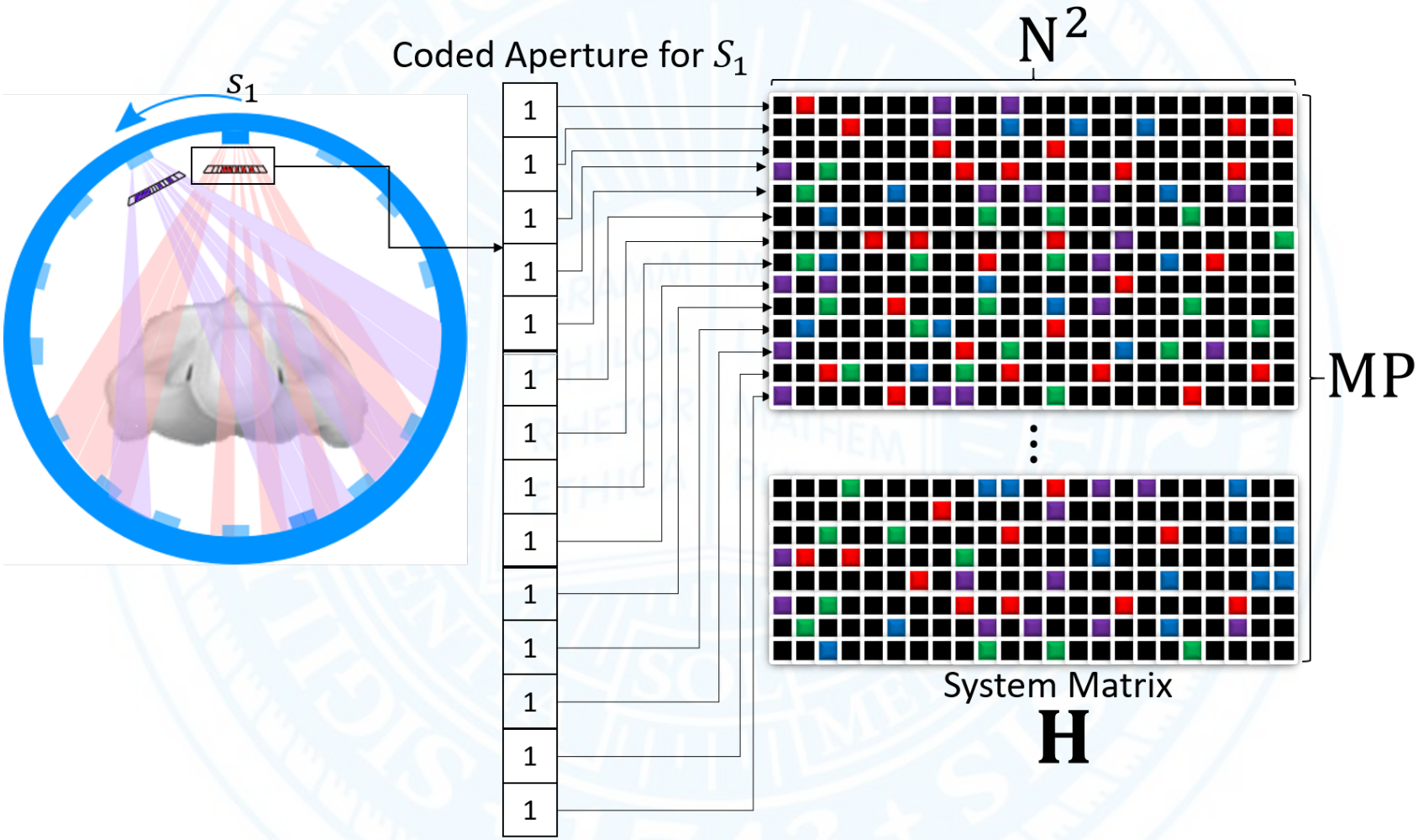

Coded aperture and energy mapping

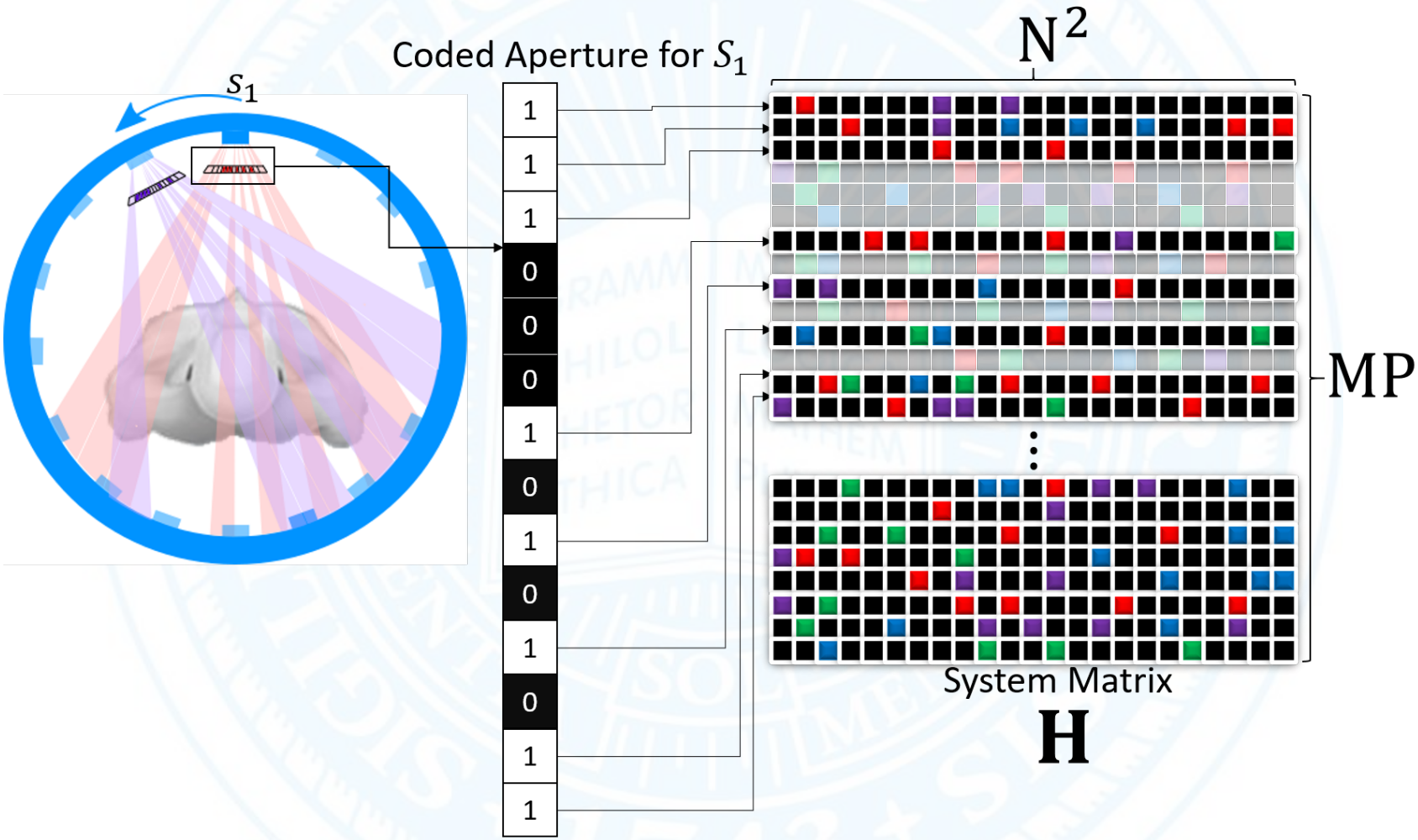

Coded aperture and energy mapping

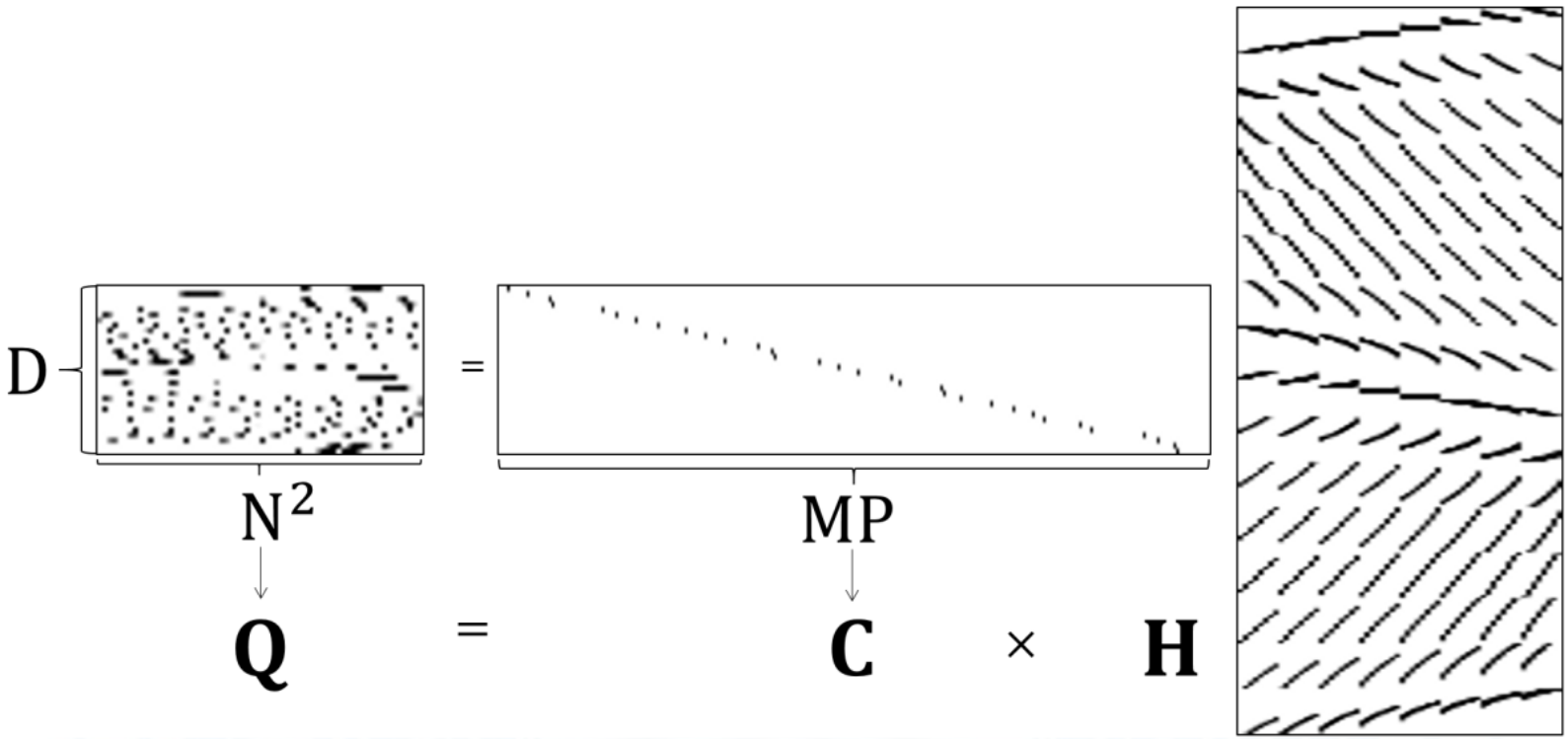

- **H**: intersection length of each ray with every pixel.
- M is the number of detector elements for each of the P view angles, N^2 is the number of pixels in the image, and D is the number of un-blocked elements in the coded apertures.
- **C**: coded aperture matrix.
- **Q**: system matrix containing the rows of **H** corresponding to the un-blocked detectors.

Coded aperture sub-sampling strategies[1]

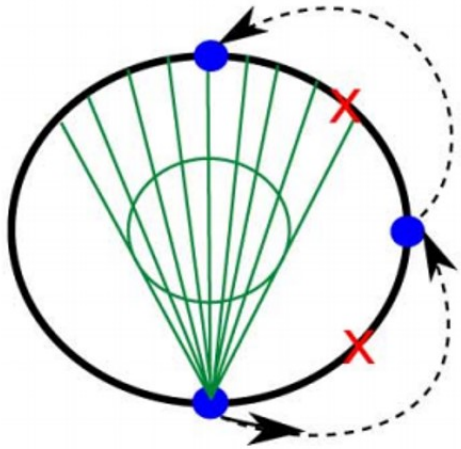

Uniform view (UV) subsampling

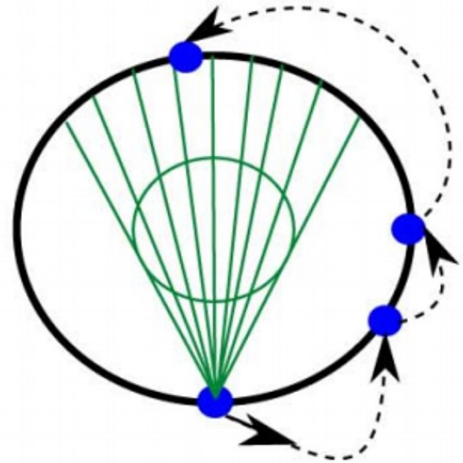

Random view (RV)-angle subsampling

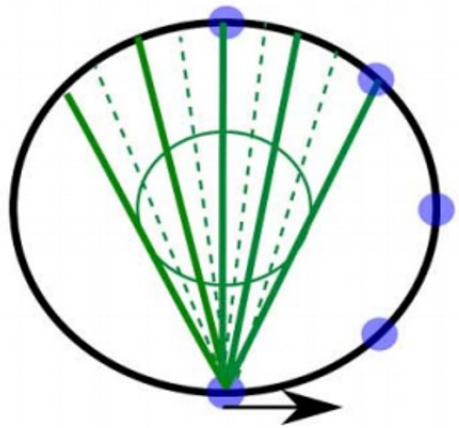

Uniform detector (UD) sampling

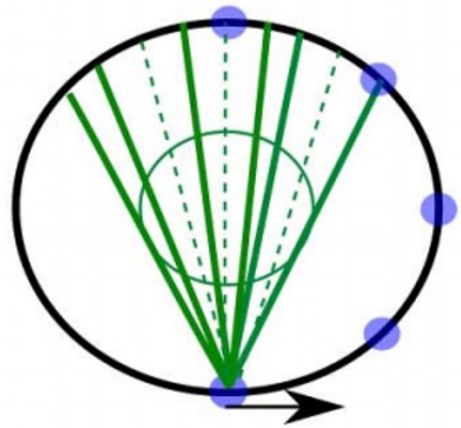

Random detector (RD) subsampling

[1] Y. Kaganovsky, D. Li, A. Holmgren, H. Jeon, K. MacCabe, D. Politte, J. O'Sullivan, L. Carin, and D. J. Brady, "Compressed sampling strategies for tomography," in JOSA A 2014.

Coded aperture optimization

The Restricted Isometry Property (RIP) δ_s of the system matrix $\tilde{\mathbf{A}} \in \mathbb{R}^{D \times N^2}$ with normalized columns is defined as:

$$(1 - \delta_s)||\mathbf{x}||_2^2 \leq ||\tilde{\mathbf{A}}\mathbf{x}||_2^2 \leq (1 + \delta_s)||\mathbf{x}||_2^2, \tag{1}$$

The matrix $\tilde{\mathbf{A}}$ satisfies the RIP if δ_s is small for reasonably large s if it holds that [2]

$$\delta_s = \max_{S \subset [N^2], |S| \leq s} ||\tilde{\mathbf{A}}_S^* \tilde{\mathbf{A}}_S - I||_2, \tag{2}$$

where $[N^2] := 1, 2, \cdots, N^2$ and $|S|$ is the cardinality of S. $\tilde{\mathbf{A}}_S$ are the column sub-matrices of $\tilde{\mathbf{A}}$ consisting of the columns indexed by S and $||\tilde{\mathbf{A}}||_2 = \left(\sum_{i=1}^{\min\{D, N^2\}} \sigma_i^2(\tilde{\mathbf{A}}) \right)^{\frac{1}{2}}$ where σ_i are the singular values of the matrix.

[2] H. Rauhut, "Compressive sensing and structured random matrices", Radon Series Comp. Appl. Math XX,2011.

Using the fact that $||\mathbf{A}||_2 \leq ||\mathbf{A}||_F$, where $||\mathbf{A}||_F = \sqrt{\sum_i \sum_j |A_{ij}|^2}$. Then (2) can be simplified as follows

$$\begin{aligned} \delta_s &= \max_{S \subset [N^2], |S| \leq s} ||\tilde{\mathbf{A}}_S^* \tilde{\mathbf{A}}_S - I||_2 \\ &\leq \max_{S \subset [N^2], |S| \leq s} ||\tilde{\mathbf{A}}_S^* \tilde{\mathbf{A}}_S - I||_F \\ &\leq ||\tilde{\mathbf{A}}^* \tilde{\mathbf{A}} - I||_F \end{aligned}$$

Therefore, δ_s is bounded by the Frobenious norm of the PSF of the system[3], $\tilde{\mathbf{A}}^* \tilde{\mathbf{A}}$, that is

$$\delta_s \leq ||\tilde{\mathbf{A}}^* \tilde{\mathbf{A}} - \mathbf{I}||_F. \tag{3}$$

[3] W. Hou and C. Zhang, "Analysis of compressed sensing based CT reconstruction with low radiation," ISPACS, Kuching, 2014.

Connection with the mutual coherence

The mutual coherence of $\mathbf{A} = [\mathbf{a}_1 \ \cdots \ \mathbf{a}_{N^2}]$ is defined as

$$\mu(\mathbf{A}) = \max_{i \neq j, 1 \leq i,j \leq N^2} \left\{ \frac{\mathbf{a}_i^T \mathbf{a}_j}{||\mathbf{a}_i||_{\ell_2} ||\mathbf{a}_j||_{\ell_2}} \right\}. \tag{4}$$

Coherence minimization can be performed by making any subset of columns in $\mathbf{A}$ as orthogonal as possible [4], that is, minimizing

$$||\tilde{\mathbf{A}}^* \tilde{\mathbf{A}} - \mathbf{I}||_F \tag{5}$$

- Result equivalent to the upper bound for the RIP in (4).
- The coded aperture optimization is formulated as the search of $\mathbf{C}$, over the $D \times MP$ binary space such that

$$\hat{\mathbf{C}} = \underset{\mathbf{C}}{\text{argmin}} \ ||\tilde{\mathbf{A}}^* \tilde{\mathbf{A}} - \mathbf{I}||_F = \underset{\mathbf{C}}{\text{argmin}} \ \Gamma. \tag{6}$$

[4] J. M. Duarte-Carvajalino and G. Sapiro, "Learning to sense sparse signals: Simultaneous sensing matrix and sparsifying dictionary optimization," in IEEE Transactions on Image Processing, 2009.

Simplification of $\tilde{\mathbf{A}}^{*}\tilde{\mathbf{A}}$

- Let $\mathbf{C} = [\mathbf{c}_1\ \mathbf{c}_2 \cdots \mathbf{c}_{MP}]$, where $\mathbf{c}_i$ are $D-$long column vectors.
- $\mathbf{W} = \mathbf{H}\mathbf{\Psi} = [\mathbf{w}_1^T\ \mathbf{w}_2^T \cdots \mathbf{w}_{MP}^T]^T$, where $\mathbf{w}_i$ are N^2- long row vectors.
- The sensing matrix $\mathbf{A}$ can be represented as

$$\mathbf{A} = \mathbf{C}\mathbf{W} = \sum_{i=1}^{MP} \mathbf{c}_i \mathbf{w}_i \tag{7}$$

- The element of $\mathbf{A}$ in the (m, n) position can be written as

$$\mathbf{A}(m, n) = \sum_{i=1}^{MP} \mathbf{c}_i(m) \mathbf{w}_i(n) \tag{8}$$

Simplification of $\tilde{\mathbf{A}}^{*}\tilde{\mathbf{A}}$

The inner product between the m^{th} and n^{th} columns after normalization of $\mathbf{A}$ is given by:

$$[\tilde{\mathbf{A}}^{T}\tilde{\mathbf{A}}]_{mn} = \frac{\sum_{i,j}^{MP}\langle \mathbf{c}_i, \mathbf{c}_j\rangle \mathbf{w}_i(m)\mathbf{w}_j(n)}{\sqrt{\left(\sum_{i,j}^{MP}\langle \mathbf{c}_i, \mathbf{c}_j\rangle \mathbf{w}_i(m)\mathbf{w}_j(m)\right)}\sqrt{\left(\sum_{i,j}^{MP}\langle \mathbf{c}_i, \mathbf{c}_j\rangle \mathbf{w}_i(n)\mathbf{w}_j(n)\right)}}. \tag{9}$$

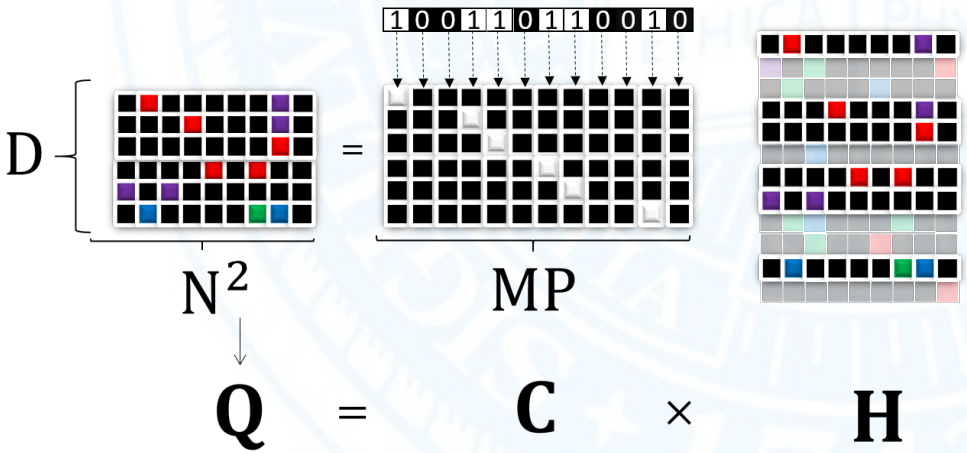

- $\langle \mathbf{c}_i, \mathbf{c}_j\rangle = 0 \quad \forall i \neq j$
- $\langle \mathbf{c}_i, \mathbf{c}_j\rangle = 1 \quad \forall i = j$ and $\mathbf{c}_i \neq \mathbf{0}$
- Thus, the norm of $\mathbf{c}_i$ can be expressed as a binary variable $b_i = \langle \mathbf{c}_i, \mathbf{c}_i\rangle$.

Simplification of $\tilde{\mathbf{A}}^{*}\tilde{\mathbf{A}}$

Simplifying (9)

$$[\tilde{\mathbf{A}}^{T}\tilde{\mathbf{A}}]_{mn} = \frac{\sum_{i=1}^{MP} b_i \mathbf{w}_i(m)\mathbf{w}_i(n)}{\left(\sum_{i=1}^{MP} b_i \mathbf{w}_i(m)\mathbf{w}_i(m)\right)^{1/2}\left(\sum_{i=1}^{MP} b_i \mathbf{w}_i(n)\mathbf{w}_i(n)\right)^{1/2}}. \tag{10}$$

- $R_i^{m,n} = \mathbf{w}_i(m)\mathbf{w}_i(n)$
- $d(m,n) = \sum_{i=1}^{MP} b_i R_i^{m,n}$
- Substituting in (10)

$$[\tilde{\mathbf{A}}^{T}\tilde{\mathbf{A}}]_{mn} = \frac{d(m,n)}{(d(m,m))^{1/2}\,(d(n,n))^{1/2}} \tag{11}$$

Optimization Cost Function

The reparameterized cost function can be formulated in terms of the parameter $\mathbf{b} = [b_1, \cdots, b_{MP}]$ as follows

$$\begin{aligned} \hat{\mathbf{b}} &= \underset{\mathbf{b}}{\operatorname{argmin}} \sum_{m=1}^{N^2} \sum_{n=1}^{N^2} |[\tilde{\mathbf{A}}^T \tilde{\mathbf{A}}]_{mn} - \mathbf{I}_{mn}|^2 \qquad (12) \\ &= \underset{\mathbf{b}}{\operatorname{argmin}} \sum_{m<n} \left(\frac{d(m,n)}{(d(m,m))^{1/2} (d(n,n))^{1/2}} \right)^2 = \underset{\mathbf{b}}{\operatorname{argmin}}\ F(\mathbf{b}) \ , \end{aligned}$$

- Values b_i can only take values 0 or 1 $\Rightarrow$ Combinatorial optimization.
- Gradient information to explore the search space cannot be used.

Optimization Cost Function

- Bound-constrained optimization can be further reduced to an unconstrained optimization problem using the following parametric transformation

$$b_i = \frac{1 + \cos\theta_i}{2}, \tag{13}$$

- Thus, the re-parameterized cost function in terms of $\boldsymbol{\theta}$ is formulated as

$$F(\boldsymbol{\theta}) = \sum_{m<n} \left(\frac{\sum_{i=1}^{MP} \frac{\cos\theta_i + 1}{2} R_i^{m,n}}{\sqrt{\left(\sum_{i=1}^{MP} \frac{\cos\theta_{i+1}}{2} R_i^{m,m}\right)} \sqrt{\left(\sum_{i=1}^{MP} \frac{\cos\theta_{i+1}}{2} R_i^{n,n}\right)}} \right)^2. \tag{14}$$

Gradient Descent Formulation

- Let

$$d_\theta(m,n) = \sum_{i=1}^{MP} \frac{1+\cos\theta_i}{2} R_i^{m,n} \tag{15}$$

then (14) can be simplified to

$$F(\boldsymbol{\theta}) = \sum_{m<n} \left(\frac{d_\theta(m,n)}{\left(d_\theta(m,m)\right)^{1/2} \left(d_\theta(n,n)\right)^{1/2}} \right)^2. \tag{16}$$

- The steepest-descent method is used to optimize (16).

Gradient Descent Formulation

- The gradients $\nabla F(\boldsymbol{\theta})_{\boldsymbol{\theta}}$ can be obtained as follows

$$\nabla F(\boldsymbol{\theta}) = \sum_{m<n} \frac{-d_\theta(m,n)\underline{\mathbf{R}}^{mn}}{d_\theta(m,m)d_\theta(n,n)} + \frac{d_\theta(m,n)^2\underline{\mathbf{R}}^{mm}}{2d_\theta(m,m)^2 d_\theta(n,n)} + \frac{d_\theta(m,n)^2\underline{\mathbf{R}}^{nn}}{2d_\theta(m,m)d_\theta(n,n)^2} \odot \sin(\theta),$$

- $\nabla F(\boldsymbol{\theta}) \in \mathbb{R}^{MP\times 1}$
- $\odot$ is the element-by-element multiplication operator
- $\underline{\mathbf{R}}^{mn} = [R_1^{mn}, R_2^{mn}, \cdots, R_{MP}^{mn}]^T$

Gradient Descent Formulation

The random stochastic gradient descent algorithm uses a sample noise term r drawn uniformly from the unit sphere. Assuming $\boldsymbol{\theta}^k$ is the k^{th} iteration result, at the $k^{th}+1$ iteration and a step size α:

$$\theta_i^{k+1} = \theta_i^k - \alpha \left[\nabla F(\theta_i^k) + r\right] \tag{17}$$

- Gray-valued coded aperture masks with pixel values between 0 and 1 which make the coded aperture fabrication impractical.
- A global threshold parameter $0 \leq t_m \leq 1$ to quantize values as

$$\beta_i = U\left(\sqrt{\frac{\cos(\theta_i)+1}{2}} - t_m\right), \tag{18}$$

- $U(x) = 1$ for $x \geq 0$, $U(x) = 0$ otherwise. Heaviside/ step function of x.
- The coded aperture matrix **C** is constructed such that matrix **Q** is formed by the rows of matrix **H** corresponding to the detector elements for which $\beta_i = 1$.

Regularization

- Global thresholding is sub-optimal.
- Transmittance of the coded apertures obtained by the optimization algorithm cannot be controlled.
- Incorporate prior knowledge about the solution by constraining the solution space through regularization terms.

$$\hat{\mathbf{b}} = \underset{\mathbf{a}}{\operatorname{argmin}}\ F(\mathbf{b}) + \gamma_1 V_1(\mathbf{b}) + \gamma_2 V_2(\mathbf{b}), \tag{19}$$

- $F(\mathbf{b})$ is the data fidelity term
- V_1 and V_2 are the regularization terms used to reduce the solution space and constrain the optimized results.
- γ_1 and γ_2 regularization weights.

Quadratic Penalty-Obtain near-binary gray codes

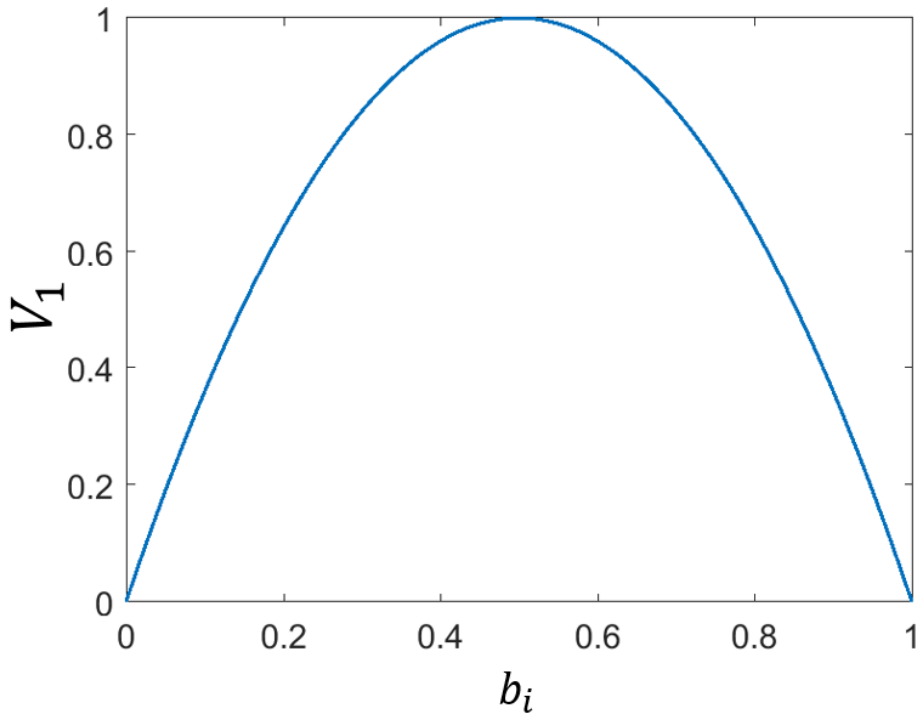

(a)

- The quadratic penalty term is

$$V_1(\mathbf{b}) = 4\mathbf{b}^T(\mathbf{1} - \mathbf{b}), \quad (20)$$

- For each coded aperture element $V_1(b_i) = 1 - (2b_i - 1)^2$.
- The penalty is maximum for $b_i = 0.5$ and minimum for 0 and 1.
- The gradient of $V_1(\mathbf{b})$ is given by $\nabla V_1(\mathbf{b}) = (-8\mathbf{a} + 4)$

Transmittance-Uniformity Penalty

The quadratic penalty term is chosen as the variance of the sum of the length of the rays that measure each pixel:

$$V_2(\mathbf{b}) = \frac{1}{N_C} \sum_{k \in \Omega_C} \left[\left(\sum_{i=1}^{MP} \sqrt{b_i} \mathbf{H}_{i,k} \right) - \mu \right]^2, \tag{21}$$

- μ desired mean for the ray concentration, N_C number of pixels in ROI Ω_C and $H_{i,k}$ is the intersection length of the i^{th} ray with every pixel inside Ω_C.
- This penalty is minimum when the number of rays that sense every pixel inside Ω_C is approximately μ.
- $\nabla V_2(\mathbf{a})$ can be obtained as follows

$$\nabla V_2(\mathbf{b}) = \frac{1}{N_C} \left[\sqrt{\mathbf{b}^T} \mathbf{H}_{\Omega_C} - \mu \right] [\mathbf{H}_{\Omega_C}]^T \odot \left[\sqrt{\mathbf{b}^T} \right]^{-1} \tag{22}$$

Configuration

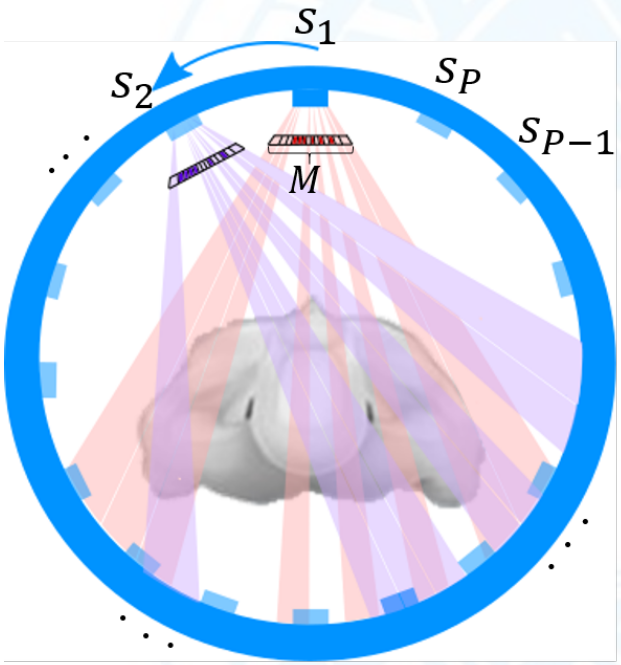

- $R_0 = 40\ cm$ → distance from the center of rotation to the X-ray source
- $T_0 = 80\ cm$ → source-to-detector-center distance
- Detector length $41.3\ cm$.
  - Case 1
    $$M = P = 2N = 64$$
  - Case 2
    $$M = P = 2N = 128$$
  - Case 3
    $$M = P = 2N = 256$$

PSNR of the Reconstructions (Case 1)

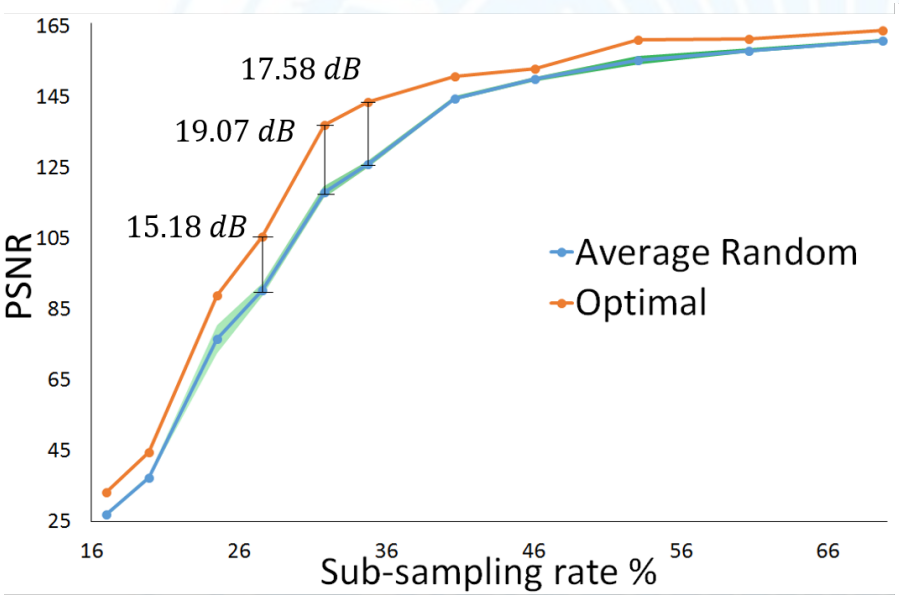

(a)

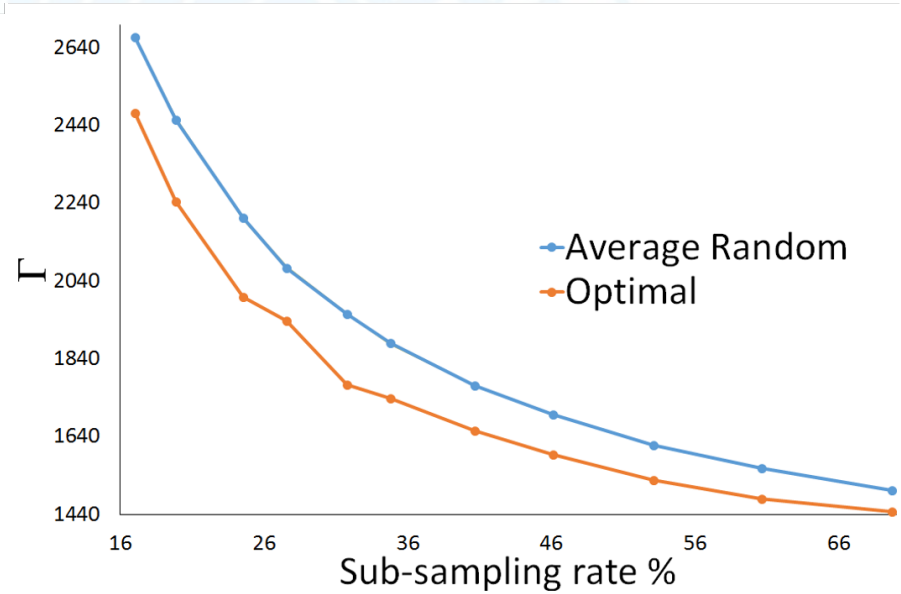

(b)

Case 1. with D=1303 unblocked rays

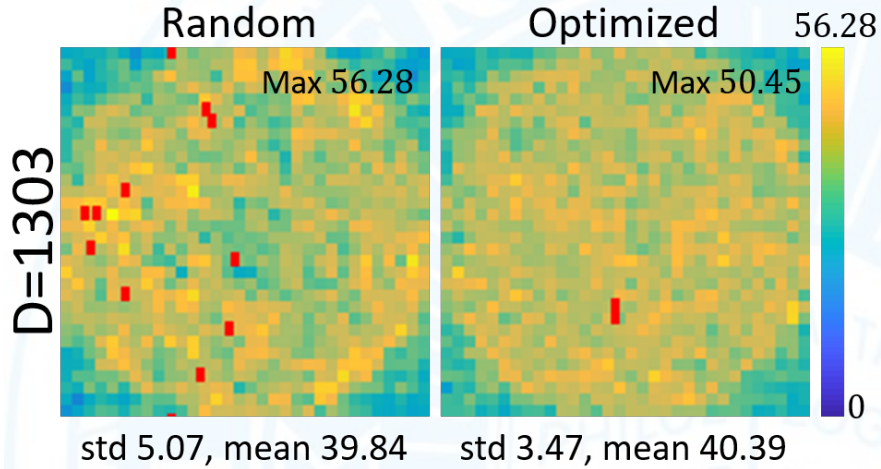

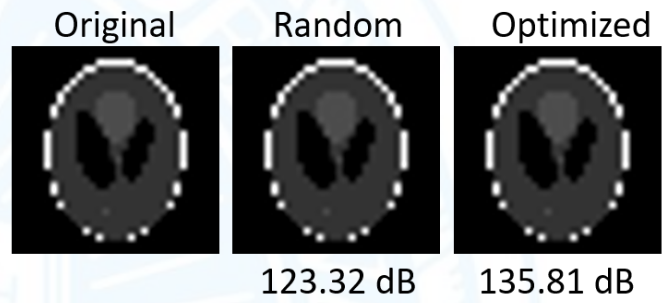

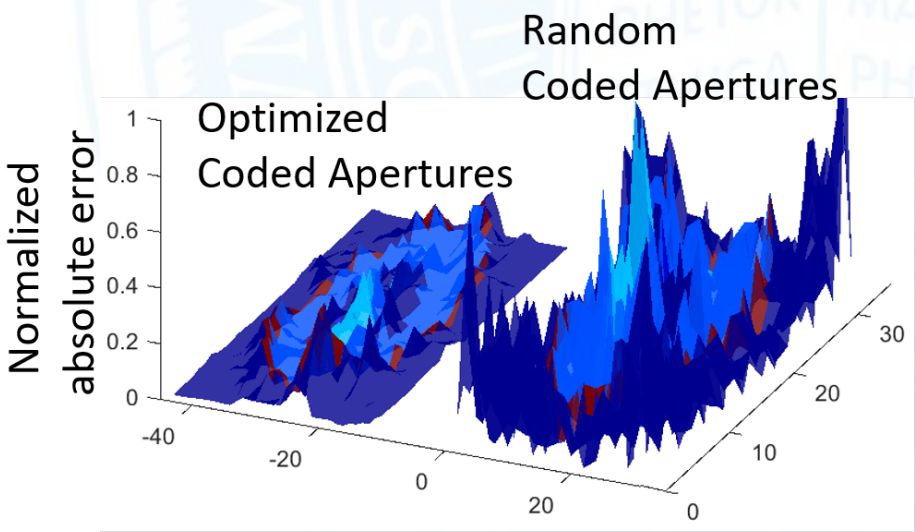

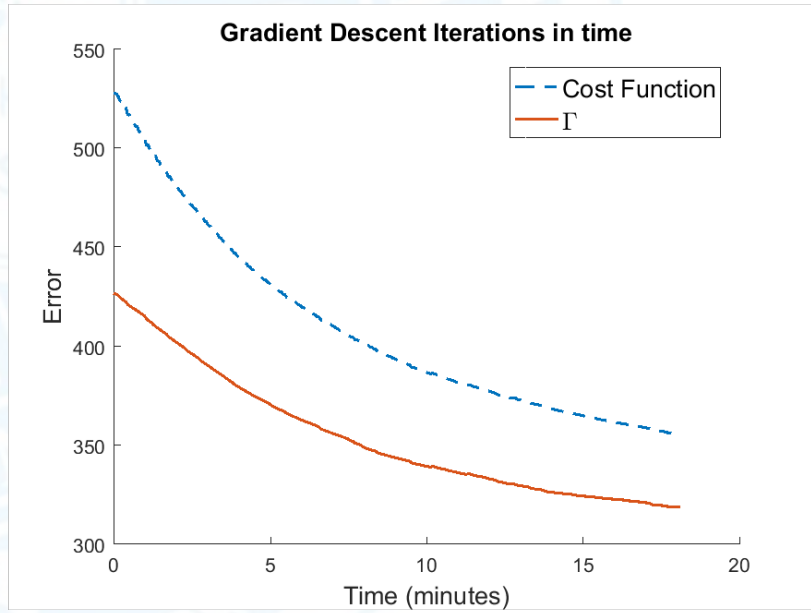

Algorithm iterations and coherence (Case 2) - Haar Wavelet

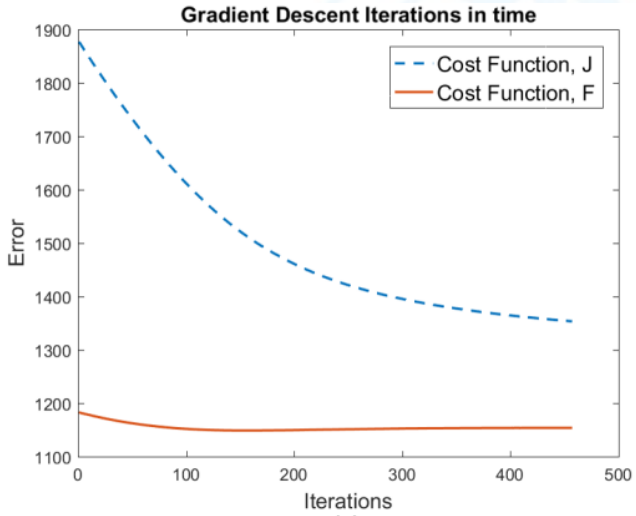

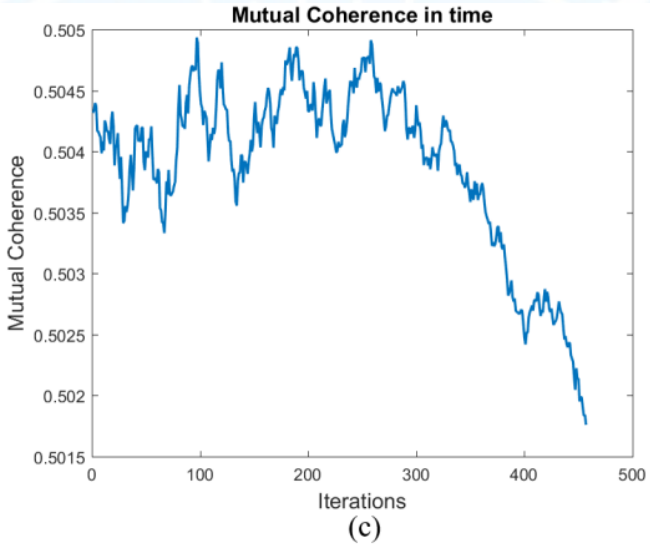

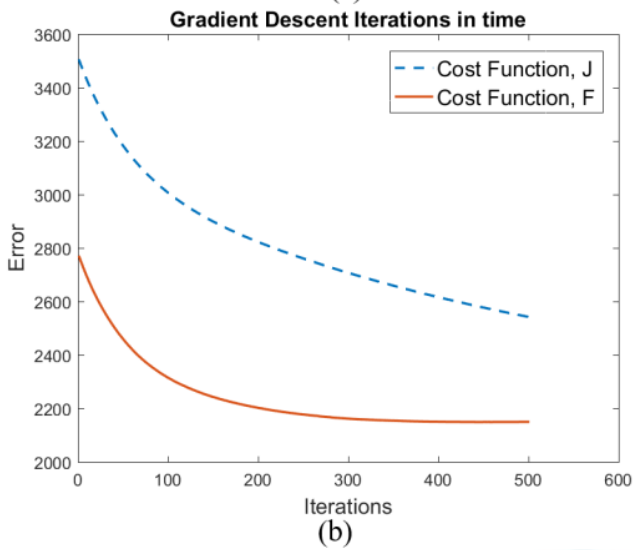

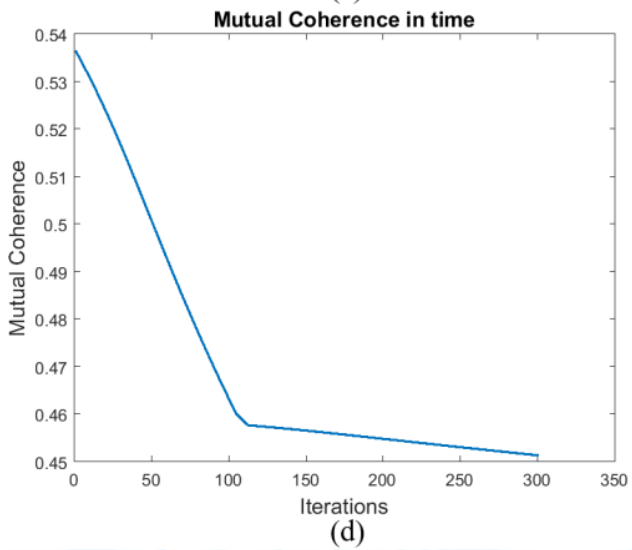

a,c Subsampling rate of 47.3%

b,d Subsampling rate of 20.3%

Reconstruction error (Case 2) for different representation basis

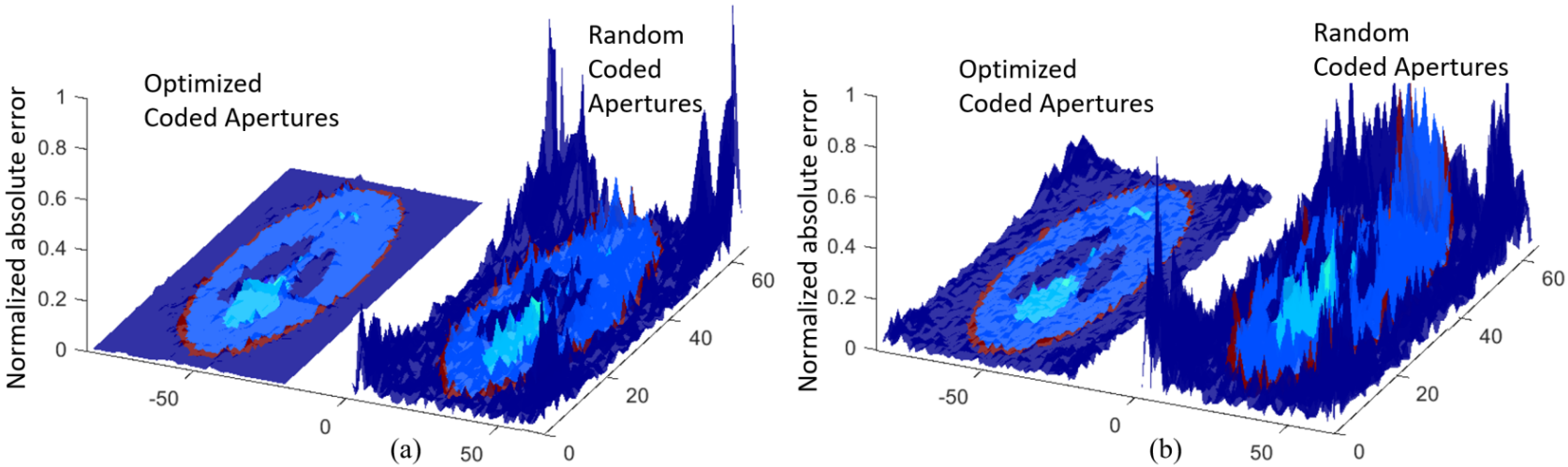

Normalized absolute error plots for the reconstructions of the 64×64 Shepp-Logan phantom.

a Haar Wavelet - Subsampling rate 32.47 %

b Symlet Wavelet Subsampling rate 32.43 %

Uniformity (Case 2)

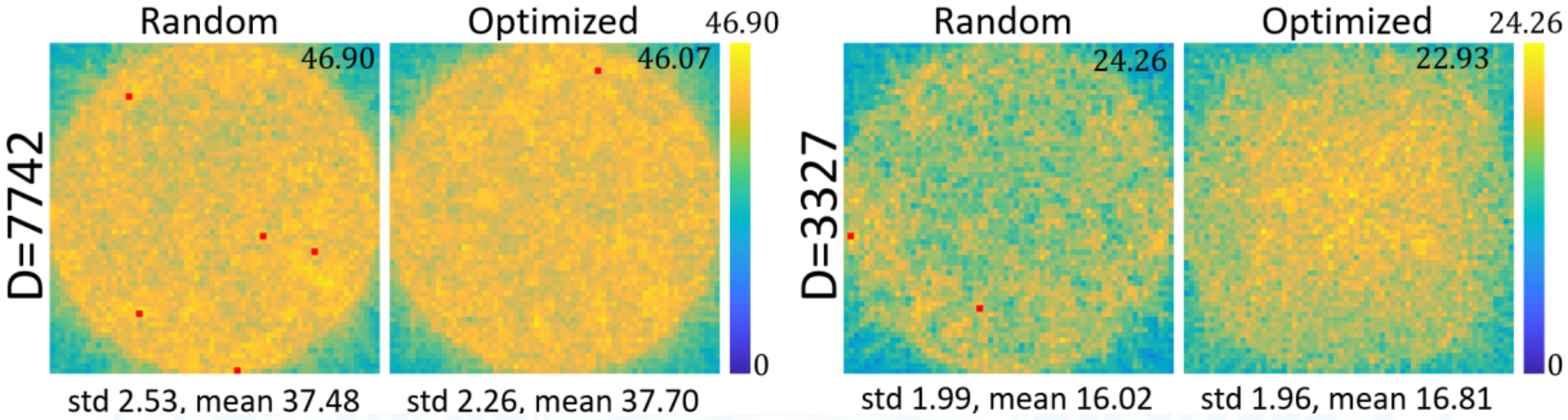

Reconstruction results (Case 2)

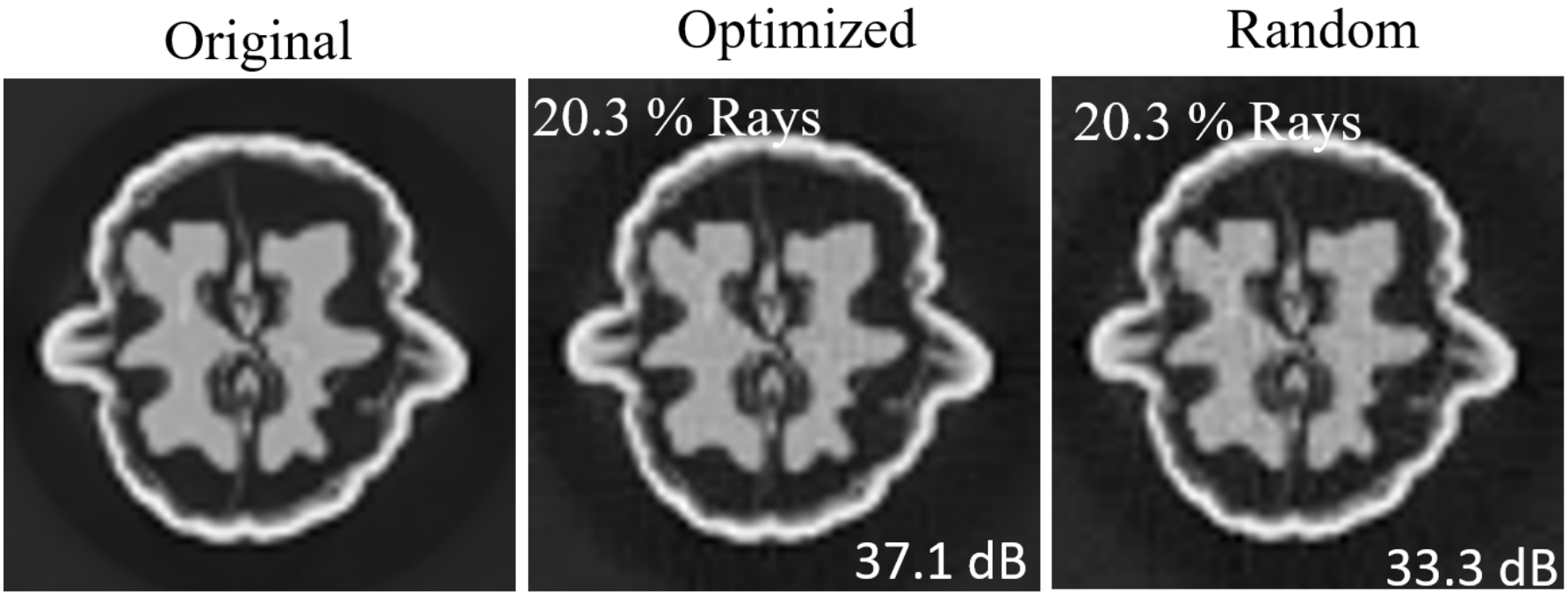

Walnut phantom - K. Hämäläinen, A. Harhanen, A. Kallonen, A. Kujanpää, E. Niemi, and S. Siltanen, "Tomographic X-ray data of a walnut," arXiv preprint arXiv:1502.04064, (2015)

Reconstruction results (Case 2)

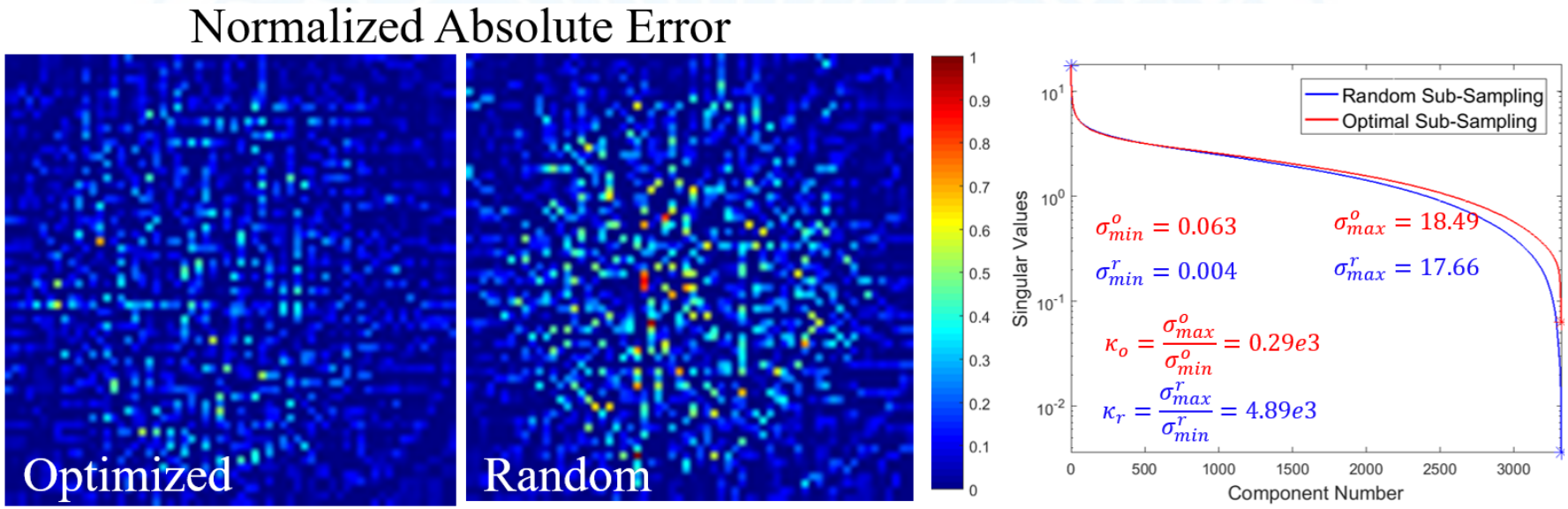

Walnut phantom - K. Hämäläinen, A. Harhanen, A. Kallonen, A. Kujanpää, E. Niemi, and S. Siltanen, "Tomographic X-ray data of a walnut," arXiv preprint arXiv:1502.04064, (2015)

Reconstruction results (Case 3) - Real projection data

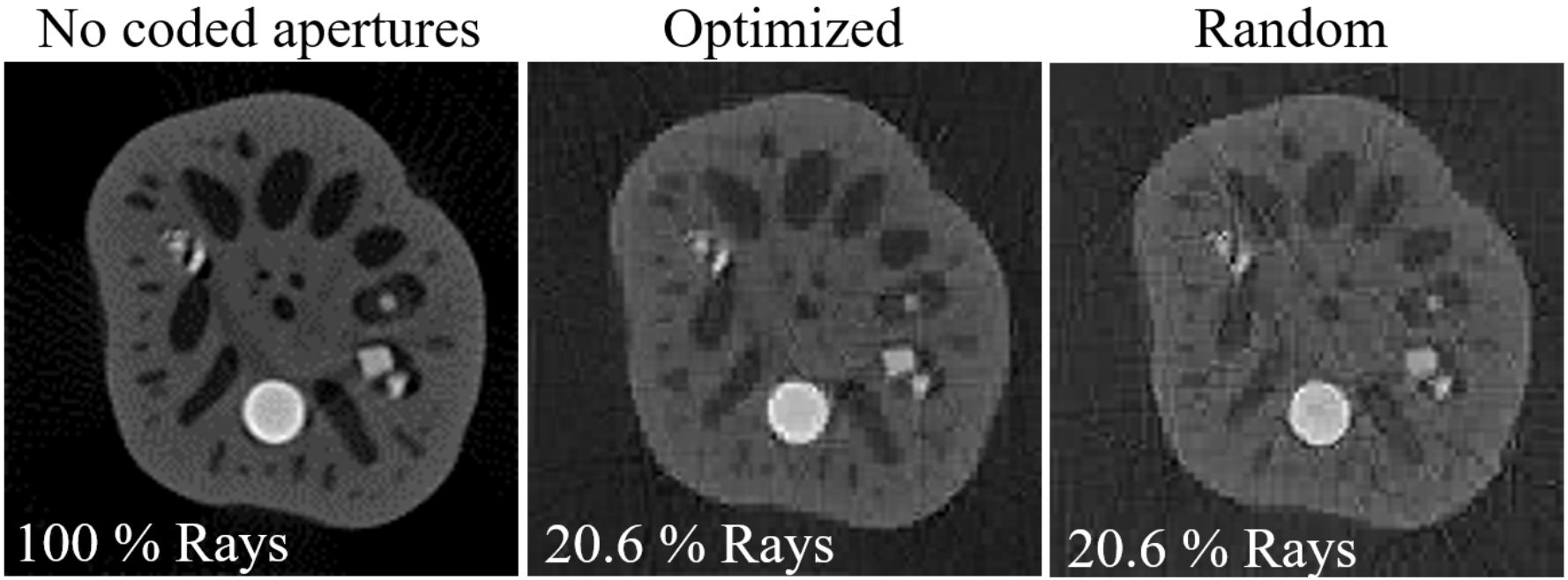

Lotus Root measurements - T. A. Bubba, A. Hauptmann, S. Huotari, J. Rimpelainen, and S. Siltanen, "Tomographic x-ray data of a lotus root filled with attenuating objects," arXiv preprint arXiv:1609.07299, (2016)

Reconstruction results (Case 3) - Real projection data

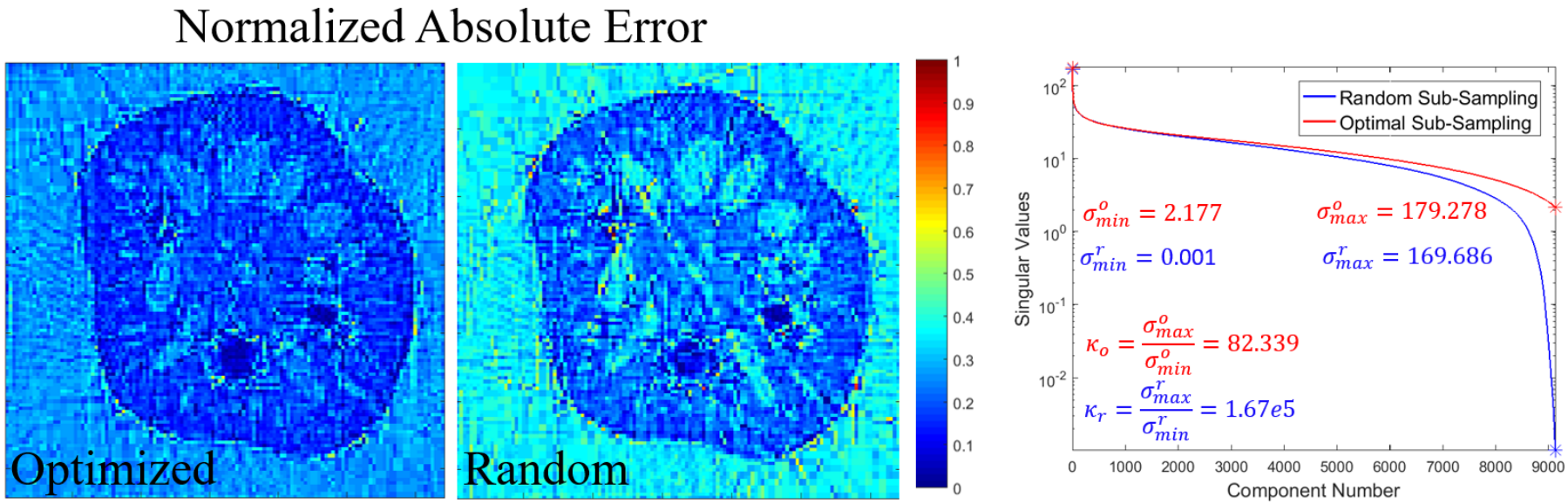

Lotus Root measurements - T. A. Bubba, A. Hauptmann, S. Huotari, J. Rimpelainen, and S. Siltanen, "Tomographic x-ray data of a lotus root filled with attenuating objects," arXiv preprint arXiv:1609.07299, (2016)

Compressive X-Ray Tomosynthesis

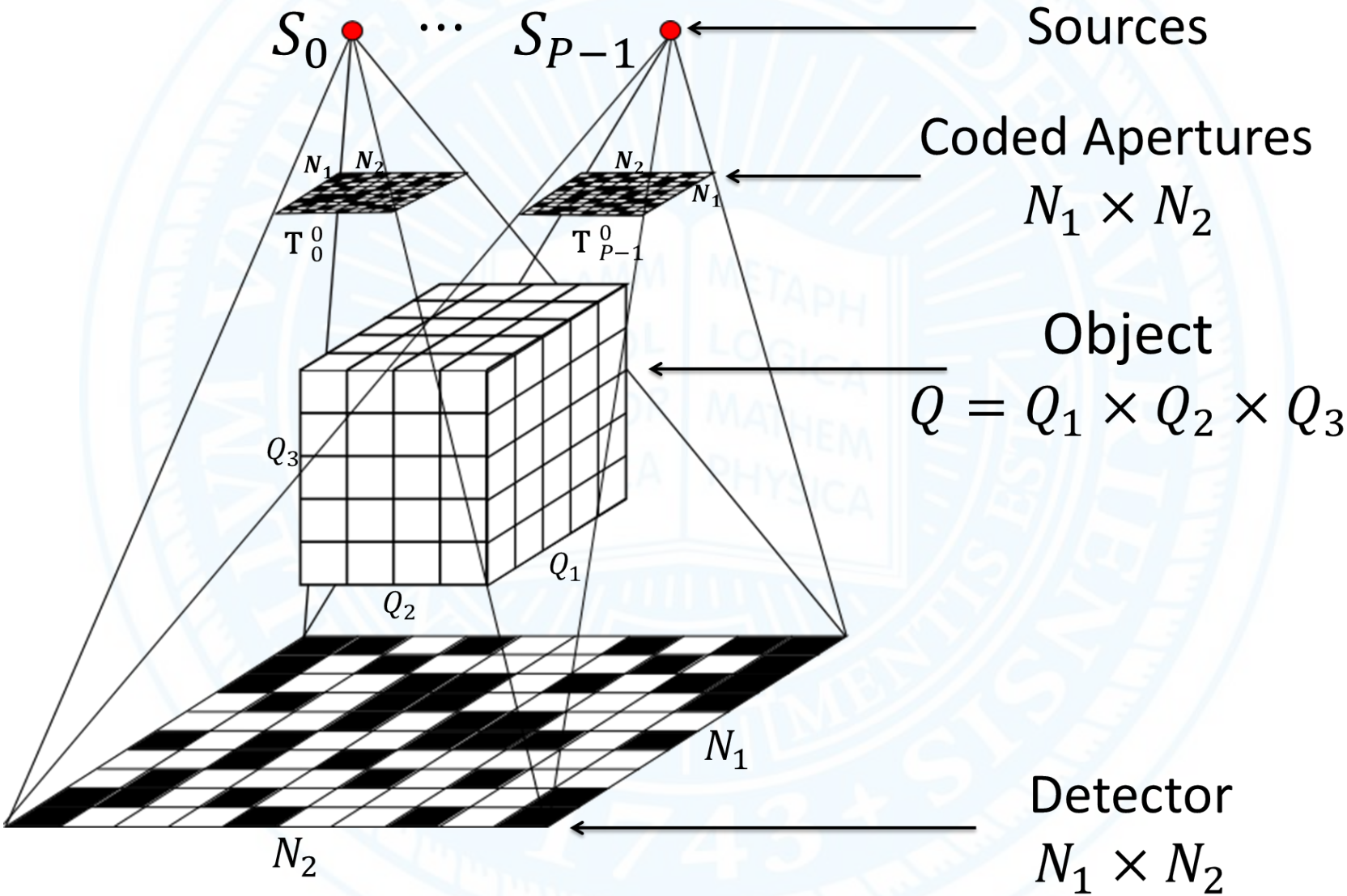

Experimental Testbed

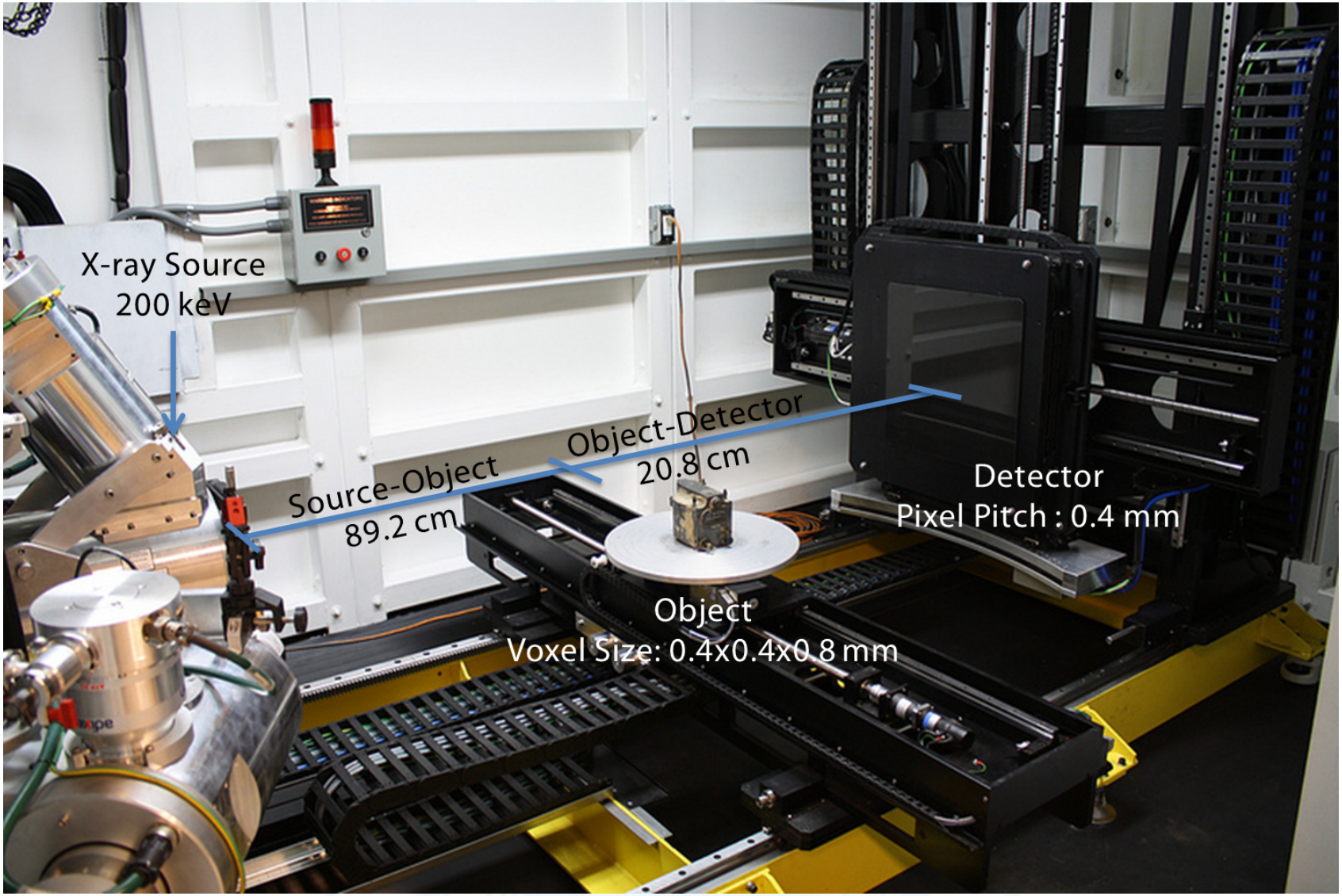

Coded Aperture Implementation

Tungsten Coded Aperture

Target (Ipod Touch)

Coded Projection

Experimental Testbed

- Sources Locations -20 cm, -10 cm, 0, 10 cm and 20 cm.
- Object: 12 slices of 128×128 pixels.
- Detector: 140×240.

Projections from 2 source locations.

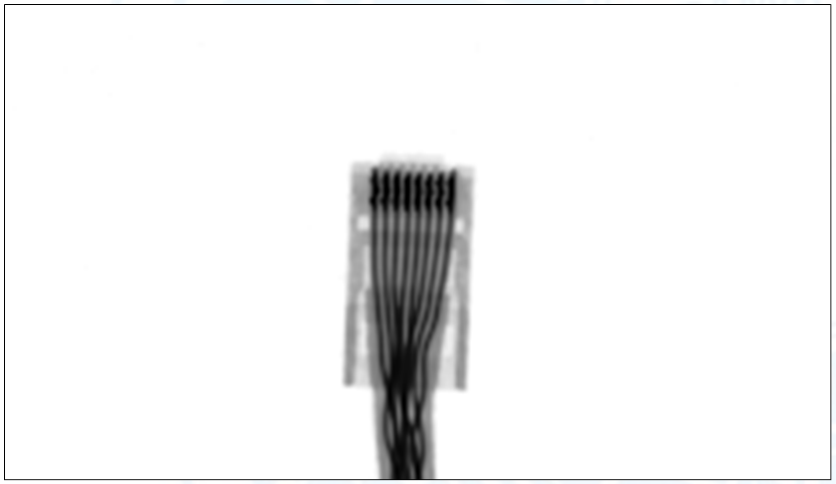

Central Source

Source located 10 cm to the left of the center source

Real Data Reconstruction - 6th Slice

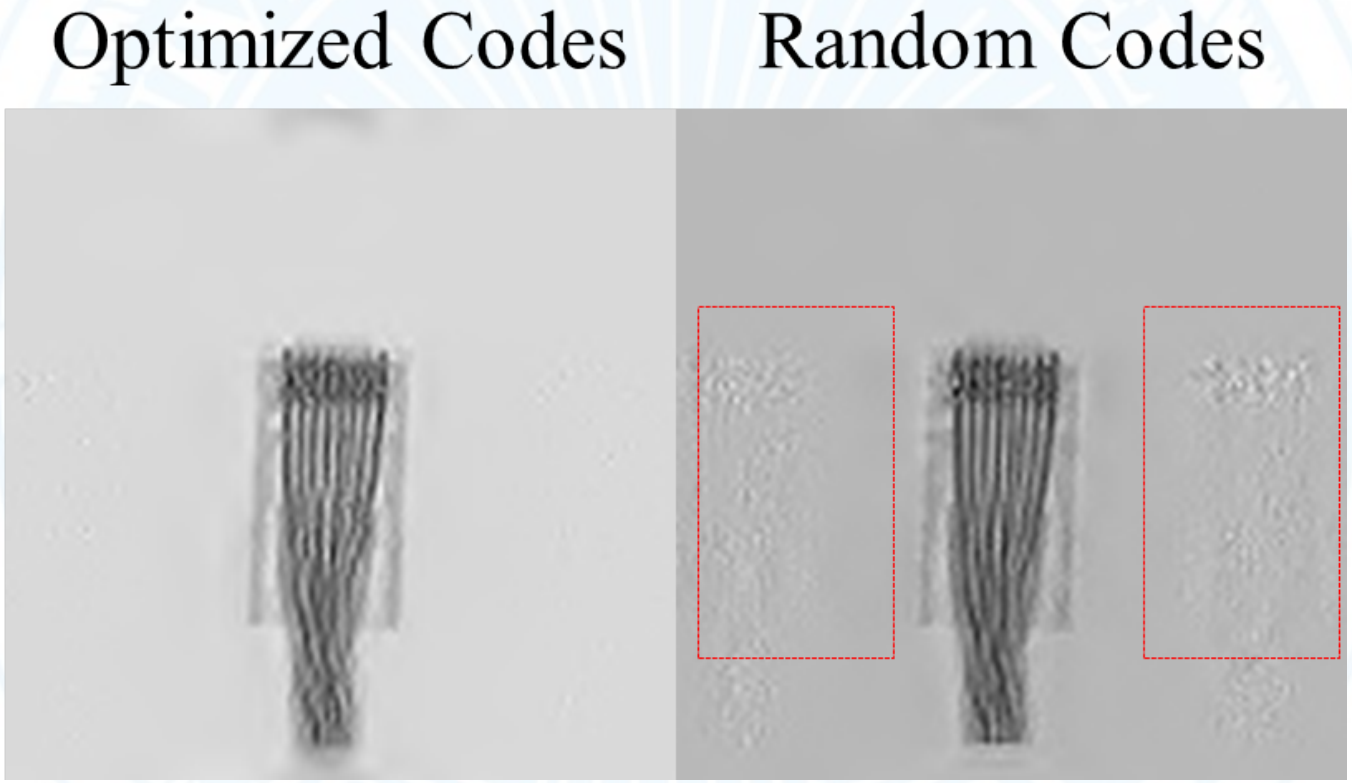

Real Data Reconstruction - 6th Slice

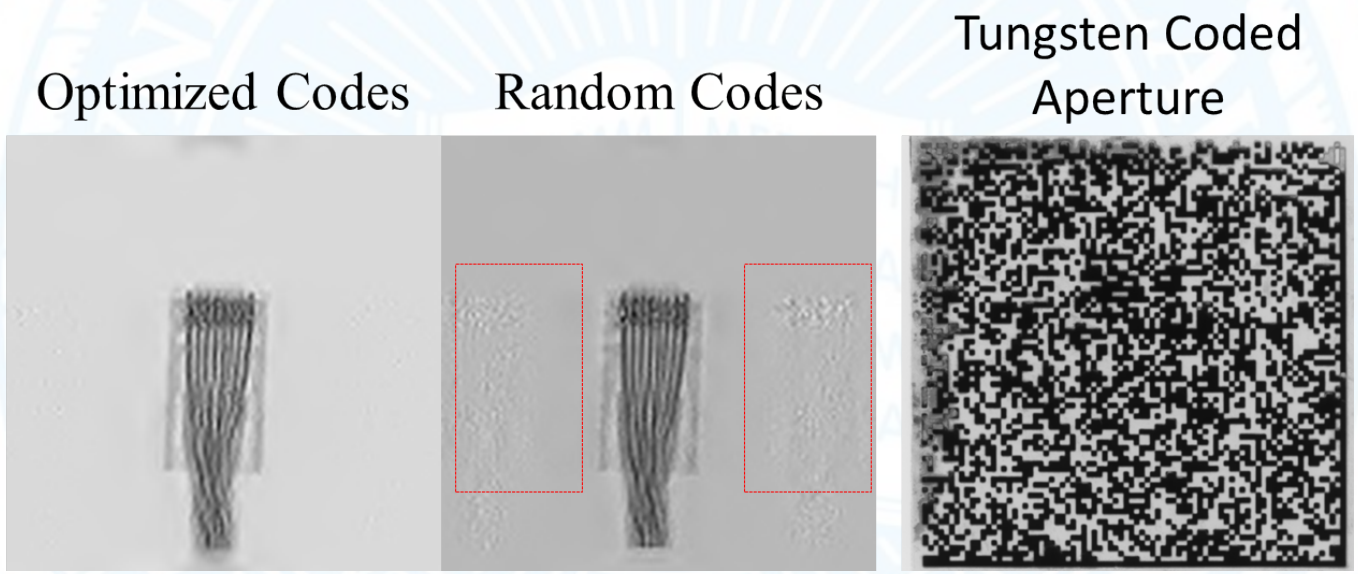

Real Data Reconstruction - 12th Slice

Optimized Codes

Random Codes

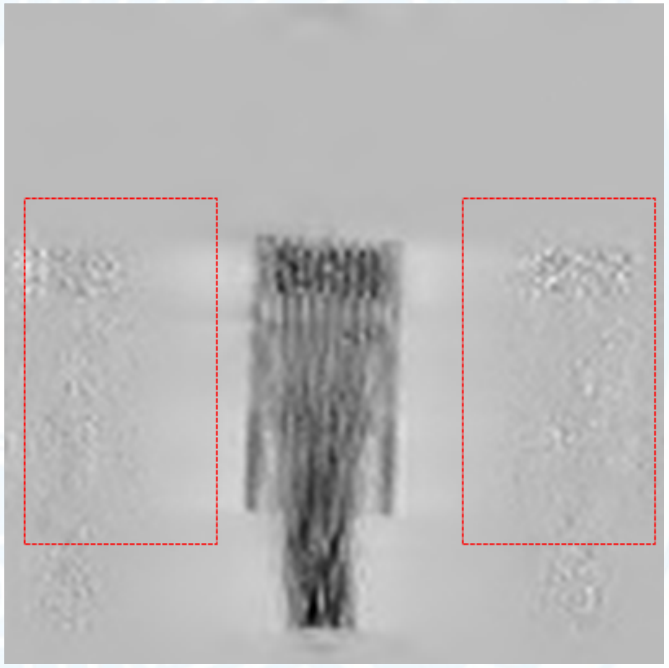

Conclusion and Future Work

- Optimized Coded apertures for compressive X-ray tomosynthesis.
- Criteria: Make each snapshot non-redundant and complimentary to each other.
- Optimization yields uniform sensing.
- Optimized codes result in 3dB PSNR improvement.
- Compressive Computed Tomography (CT).
- Compressive Spectral CT.

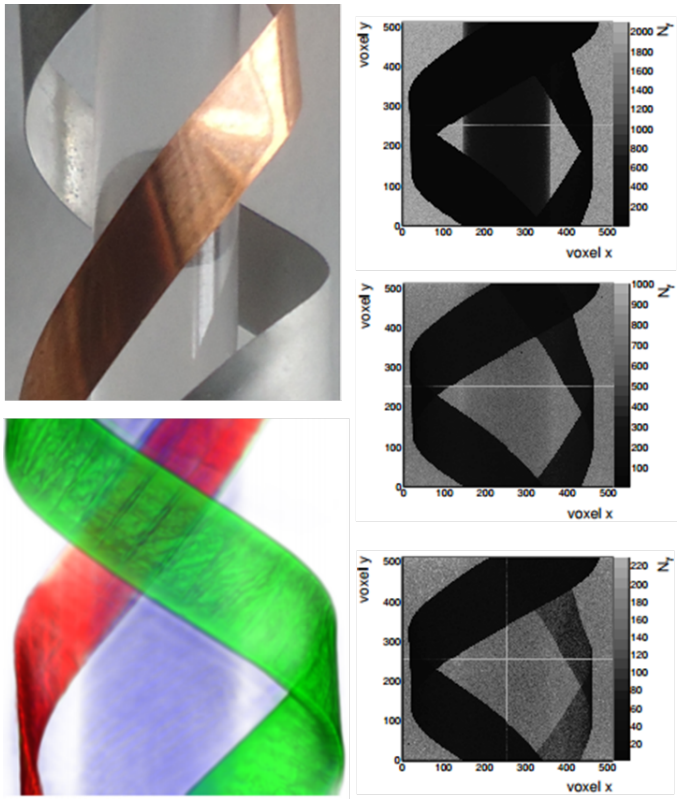

Acknowledgements

- Computational Imaging Group: Hoover Rueda, Claudia Correa, Laura Galvis, Chen Fu, Angela Cuadros, Alejandro Parada, Carlos Mendoza, Juan Becerra, Michael Don, Edgar Salazar, Juan Florez.
- Collaborators
  - Dr. Javier Garcia-Frias - University of Delaware
  - Dr. Daniel Lau - University of Kentucky, College of Engineering
  - Christopher Peitsch - Chesapeake Testing Services,Inc.
  - Dr. Clare Lau, Dr. David Laurence - JHU-APL
  - Dr. Xu Ma - Beijing Institute of Technology
  - Kris Roe - Smiths Detection
- Sponsored by the Nokia Foundation and Fulbright Finland Foundation
- Funding from